Hybrid Redox Polyethers: Molecular Melts of Metalloporphyrins

Jeffrey W. Long, Il Kwang Kim,† and Royce W. Murray*

Contribution from the Kenan Laboratories of Chemistry, University of North Carolina, Chapel Hill, North Carolina 27599-3290, and Wonkwang University, Iksan City, South Korea, 570-749

Received June 23, 1997[⊗]

Abstract: Attachment of four oligomeric (MW 550) ethylene glycol chains to tetraphenylporphyrin results in a highly viscous, room temperature melt—a hybrid redox polyether—that is highly concentrated in porphyrin sites (∼0.4 M) and will dissolve $LiClO_4$ electrolyte. Microelectrode voltammetry in undiluted, free base and Co and Fe-metalated melts yields apparent diffusion coefficients that for 1.2 M $LiClO_4$ electrolyte vary by $>10^3$-fold, from a high of 6.2×10^{-9} cm^2 s^{-1} for the ring reduction of the free base to a low of ca. 3×10^{-12} cm^2 s^{-1} for the Co(II/III) oxidation in a Co-metalated melt. Taking the latter as measuring the true physical self-diffusivity of the porphyrins, electron self-exchange rate constants are found for four porphyrinic redox couples (free base (0/1−), Co(II/I), Fe(II/I), and Fe(III/II) give 3.6×10^6, 1.2×10^5, 3.7×10^4, and 1.1×10^4 M^{-1} s^{-1}, respectively). An activation study yields large free energy activation barriers for these couples, and exponential pre-factors in the $10^{13}-10^{14}$ s^{-1} range. The polyether appendages provide a weakly coordinating "solvent" for the porphyrin centers, and the introduction of ligands like pyridine and carbon monoxide at the gas/melt interface causes changes in Fe(III/II) voltammetry consistent with axial coordination in the semisolid melt. The axial coordination and voltammetric change is reversed by removing the ligand from the bathing gas.

Ionically conductive polymers ("polymer electrolytes") consisting of polyethers with dissolved alkali metal salts[1] have been widely investigated in light of their hoped-for applications in batteries and electrochromic devices. Our laboratory has exploited polymer electrolytes as model semisolid media for a different purpose, "solid-state voltammetry", in which various attributes of voltammetry with microelectrodes are brought to bear on the study of electrochemical phenomena in these highly viscous phases.[2] For example, electroactive species can be dissolved in polyethers and their physical diffusion rates and electron transfer dynamics measured.[3]

Electroactive molecules investigated[2,3] in polymer electrolytes include ferrocenes, metal bipyridine complexes, viologens, and metalloporphyrins. As solutes in fluid solutions, the electrochemical properties of metalloporphyrins are well documented.[4,5] While examples of axial ligation chemistry[2b] and dioxygen electrocatalysis[6] have been observed for metalloporphyrins dissolved in polymer electrolytes, in general their solubilities in these media, as well as those of other interesting electroactive species, are limited. Studies of electroactive solutes in polyethers are hampered by low low solubilities, especially in exploration of ever more solid-like phases where low concentrations conspire with low diffusivities to generate small voltammetric currents. Poor solubilities of Fe(TPP)-Cl and Co(TPP)-Cl in polyether solvents are only partially addressed by using the analogous tetrakis(*o*-aminophenyl)porphyrin complexes.[7]

The meager solubilities of interesting electroactive species in polyether solvents led us (among other objectives) to attach polyethers to the redox species,[8] in the first case ferrocene. The hybrid product had its own "solvent" (the attached polyether chain) to dissolve any necessary alkali metal electrolyte (such as $LiClO_4$), and thus could be studied as an *undiluted* redox phase. Synthetic explorations of other species, including metal−bipyridines,[9a,b] methylviologen,[9c,d] tetrathiafulvalene,[9e] and metalloporphyrins,[9f] revealed further the important result that, virtually without exception, attachment of an appropriate length or number of oligomeric polyether chains produces materials that are highly viscous, concentrated, room temperature molecular *melts*, a class of materials which we term *hybrid redox polyethers*.

* Address correspondence to this author at the University of North Carolina.

† Wonkwang University.

⊗ Abstract published in *Advance ACS Abstracts,* November 1, 1997.

(1) Hara, M. In *Polyelectrolytes, Science & Technology*; Hara, M., Ed.; Marcel Dekker, Inc.: New York, 1993.

(2) (a) Wooster, T. T.; Longmire, M. L.; Zhang, H.; Watanabe, M.; Murray, R. W. *Anal. Chem.* **1992**, *64*, 1132. (b) Geng, L.; Reed, R. A.; Kim, M.-H.; Wooster, T. T.; Oliver, B. N.; Egekeze, J.; Kennedy, R. T.; Jorgenson, J. W.; Parcher, J. F.; Murray, R. W. *J. Am. Chem. Soc.* **1989**, *111*, 1614.

(3) (a) Haas, O.; Velazquez, C. S.; Porat, Z.; Murray, R. W. *J. Phys. Chem.* **1995**, *99*, 15279. (b) Che, G.; Dong, S. *Electrochim. Acta* **1993**, *38*, 2315. (c) Wooster, T. T.; Watanabe, M.; Murray, R. W. *J. Phys. Chem.* **1992**, *96*, 5886. (d) Wooster, T. T.; Longmire, M. L.; Murray, R. W. *J. Phys. Chem.* **1991**, *95*, 5315. (e) Watanabe, M.; Wooster, T. T.; Murray, R. W. *J. Phys. Chem.* **1991**, *95*, 4573. (f) Watanabe, M.; Longmire, M. L.; Murray, R. W. *J. Phys. Chem.* **199**0, *94*, 2614. (g) Longmire, M. L.; Watanabe, M.; Zhang, H.; Wooster, T. T.; Murray, R. W. *Anal. Chem.* **1990**, *62*, 747.

(4) (a) Bottomley, L. A.; Kadish, K. M. *Inorg. Chem.* **1981**, *20*, 1348. (b) Kadish, K. M.; Morrison, M. M.; Constant, L. A.; Dickens, L.; Davis, D. G. *J. Am. Chem. Soc.* **1976**, *98*, 8387. (c) Constant, L. A.; Davis, D. G. *Anal. Chem.* **1975**, *47*, 2253.

(5) (a) Huet, J.; Gaudemer, A.; Boucly-Goester, C.; Boucly, P. *Inorg. Chem.* **1982**, *21*, 3413. (b) Truxillo, L. A.; Davis, D. G. *Anal. Chem.* **1975**, *47*, 2260.

(6) Bettelheim, A.; Reed, R.; Hendricks, N. H.; Collman, J. P.; Murray, R. W. *J. Electroanal. Chem.* **1987**, *238*, 259.

(7) Reed, R. A. Ph.D. Dissertation, University of North Carolina, Chapel Hill, 1987.

(8) Pinkerton, M. J.; Mest, Y. Le; Zhang, H.; Watanabe, M.; Murray, R. W. *J. Am. Chem. Soc.* **1990**, *112*, 3730.

(9) (a) Williams, M. E.; Masui, H.; Long, J. W.; Malik, J.; Murray, R. W. *J. Am. Chem. Soc.* **1997**, *119*, 1997. (b) Long, J. W.; Velazquez, C. S.; Murray, R. W. *J. Phys. Chem.* **1996**, *100*, 5492. (c) Hatazawa, T.; Terrill, R. H.; Murray, R. W. *Anal. Chem.* **1996**, *68*, 597. (d) Terrill, R. H.; Hatazawa, T.; Murray, R. W. *J. Phys. Chem.* **1995**, *99*, 16676. (e) Velazquez, C. S.; Murray, R. W. *J. Electroanal. Chem.* **1995**, *396*, 349. (f) Velazquez, C. S.; Hutchison, J. E.; Murray, R. W. *J. Am. Chem. Soc.* **1993**, *115*, 7896. (g) Masui, H.; Murray, R. W. *Inorg. Chem.* In press.

S0002-7863(97)02081-7 CCC: $14.00

This paper extends our investigation of porphyrin-based hybrid redox polyethers beyond our preliminary[9f] report, to the synthesis and electrochemistry of undiluted polyether−porphyrin hybrid phases in which four short poly(ethylene glycol) chains (avg. MW 550) are attached to tetrakis(*p*-hydroxyphenyl)porphyrin via ether linkages.

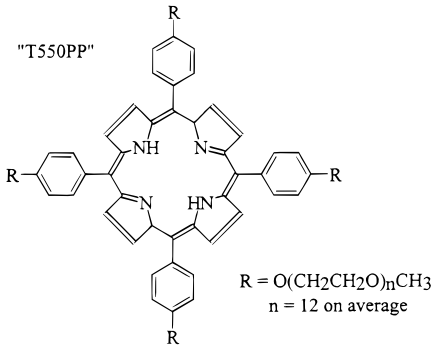

The free base tetrakis-MePEG-porphyrin, (abbrev. T550PP) is readily metalated with Fe or Co to produce the analogous metalloporphyrins Fe(T550PP)-Cl and Co(T550PP). Polyether-porphyrin derivatives have been previously prepared by other groups, but with emphasis on aggregation[10a] and thermotropic phase behavior.[10b] Our investigation focusses on the voltammetry of the undiluted, amorphous MePEG-porphyrin hybrid melt phases, analyzing the results for diffusion coefficients and porphyrin electron self-exchange rate constants, and demonstrating that voltammetrically detectable changes in the axial coordination in a semisolid Fe(T550PP)-Cl melt can be effected by partition of gaseous ligands like CO and pyridine into the porphyrin phase, and that these coordination changes are reversible.

The present electrochemical investigation is the first for undiluted porphyrin melt phases**,** and represents a beginning for semi-solid state porphyrin electron transfer dynamics and axial coordination chemistry.

Experimental Section

Chemicals. Dimethylformamide (Mallinkrodt) was distilled from 4 Å molecular sieves under reduced pressure. Monomethyl terminated oligomeric ethylene glycol (MW 550, MePEG550, Aldrich) was dried under vacuum at 70 °C for 24 h. $LiClO_4$ was recrystallized from methanol and dried under vacuum at 70 °C for 2 days. All other chemicals were used as received.

Analysis. ^{1}H NMR spectra were recorded on a Bruker AC-250 MHz instrument, UV−visible spectra on a Unicam UV4 spectrometer, and differential scanning calorimetry on a Seiko DSC 220-CU (at 10 °C/min). Elemental analysis was performed by Galbraith Laboratories, Knoxville, TN.

Preparation of MePEG550-Tosylate. Modifying a method by Gokel et al.,[11] a solution of 7.79 g (0.0142 mol) of MePEG550 in 20 mL of pyridine was added slowly dropwise (over 30 min) to a solution of 3.00 g (0.0157 mol) of *p*-tosyl chloride in 20 mL of pyridine at 5 °C. The reaction mixture was held at 5 °C with stirring for 2 h, and then warmed to room temperature and stirred for an additional 8 h, following which it was added to 100 mL of cold water. The water layer was extracted with two 75-mL portions of dichloromethane, which were combined and extracted with three 75-mL portions of 6 N HCl. The organic layer was dried over sodium sulfate and 4 Å molecular sieves, and the dichloromethane was removed by evaporation in vacuo. NMR (^{1}H, in acetone-d_6): δ (ppm) 2.45 (s, 3H), 3.33 (s, 3H), 3.4−3.6 (multiplet, 44H), 3.66 (t, 2H), 4.18 (t, 2H), 7.50 (d, 2H), 7.08 (d, 2H).

Synthesis of Tetrakis(*p*-MePEG550-phenyl)porphyrin (T550PP). To 200 mL of dimethylformamide was added 0.500 g (0.000737 mol) of tetrakis(*p*-hydroxyphenyl)porphyrin (Porphyrin Products, Logan, UT), 2.70 g (0.00380 mol, an excess) of MePEG550-tosylate, and 10 g of potassium carbonate. The mixture was vigorously degassed with nitrogen, then heated to reflux under N_2 for 32 h, cooled, and filtered, and the solvent was removed by vacuum evaporation, leaving a mixture of a solid and a dark oil. The mixture was extracted with 100 mL of dichloromethane, giving a dark purple solution that was filtered and the dichloromethane that was evaporated. The remaining purple oil was loaded onto a flash chromatography column containing neutral alumina, eluting a tight purple band with a mixture of 5% pyridine and 95% acetonitrile. The collected band was dried in vacuo, giving a final dark purple oil product, at a reaction yield of approximately 25%. NMR (in CD_2Cl_2): δ (ppm) 3.30 (s, 3H), 3.4−3.8 (multiplet, 43H), 4.02 (t, 2H), 4.44 (t, 2H), 7.32 (d, 2H), 8.12 (d, 2H), 8.90 (s, 2H). UV−visible: CH_2Cl_2, λ_{MAX}/nm (ϵ/M^{-1} cm^{-1}), 422 (212000), 518 (14900), 558 (9930), 596 (4370), 650 (5410). Elemental analysis: calcd, C 60.89, H 8.16, N 1.69, O 29.28; found, C 59.89, H 8.09, N 1.97, O 29.40. Differential scanning calorimetry (DSC): T_G, −56 °C; T_C, −33 °C; T_M, 7 °C.

Synthesis of Co[tetrakis(*p*-MePEG550-phenyl)porphyrin], Co-(T550PP). To 80 mL of dimethylformamide was added 0.264 g (0.000094 mol) of tetrakis(*p*-MePEG550-phenyl)porphyrin, 0.0610 g (0.00047 mol, an excess) of copper(II) chloride, and 0.0771 g (0.00094 mol) of sodium acetate. The thoroughly degassed solution was then refluxed for 48 h under N_2, cooled, and filtered, and the solvent was removed by vacuum evaporation. Redissolving the product in acetonitrile and filtering again, the product was eluted as a reddish-brown band from a neutral alumina column with a solution of 10% methanol and 90% acetonitrile. The product was collected and the solvents evaporated in vacuo, giving a reddish-orange oil. UV−visible: CH_2Cl_2, λ_{MAX}/nm (ϵ/M^{-1} cm^{-1}), 414 (199 000), 532 (11 800). Elemental analysis: calcd, C 59.63, H 7.99, N 1.66, O 28.67, Co 2.03; found, C 58.86, H 7.80, N 1.77, O 28.78, Co 1.87. DSC: T_G, −55 °C; T_C, −35 °C; T_M, 6 °C.

Synthesis of Fe[tetrakis(*p*-MePEG550-phenyl)porphyrin]Cl, Fe(T550PP)-Cl. To 80 mL of dimethylformamide was added 0.264 g (0.000094 mol) of tetrakis(*p*-MePEG550-phenyl)porphyrin, 0.0762 g (0.00047 mol) of $FeCl_3$, and 0.0771 g (0.00094 mol) of sodium acetate. The solution was degassed and refluxed for 48 h, then filtered, and the dimethylformamide was removed by vacuum evaporation. The product was redissolved in acetonitrile, filtered, and then eluted from a neutral alumina column as a green band with a solvent mixture of 10% methanol and 90% acetonitrile. This band was collected and the solvents were removed by evaporation, giving a green oil. Four drops of concentrated HCl was added and the mixture was stirred for 20 min, by which time the oil had turned to brownish-red. The excess HCl and water were removed by vacuum evaporation at 70 °C for 2 days. UV−visible: CH_2Cl_2, λ_{MAX}/nm (ϵ/M^{-1} cm^{-1}), 386 (53 000), 422 (107 000), 52 (11 700), 700 (2 750). Elemental analysis: calcd, C 59.02, H 7.84, N 1.64, O 28.38, Fe 1.90; found, C 57.20, H 7.80, N 1.77, O 28.58, Fe 1.67. DSC: T_G, −55 °C; T_C, −31 °C; T_M, 7 °C.

Preparation of Films and Electrodes. Voltammetry and chronoamperometry were performed with either 10 or 25 μm diameter microdisk working electrodes. The cell platform was fashioned as before[12] from a 10 or 25 μm diameter Pt wire, 0.5 mm silver wire (quasi-reference electrode), and 24 gauge Pt wire (counter electrode), potted together in a 6 mm diameter cylinder of Epon 825 resin (Shell). Films, typically 200 μm thick, of the polyether-porphyrins were cast onto the electrode platform from methanolic solutions containing the desired amount of $LiClO_4$ electrolyte. The methanol was evaporated under a stream of nitrogen and the electrode assembly dried in a sealed, jacketed glass cell at 70 °C under vacuum for 36 h before measurements were obtained. All measurements were performed at temperatures above the glass and melting transitions, so that the polyether-porphyrin was always in its amorphous melt phase.

Most measurements were obtained with the electrochemical cell under active vacuum. Carbon monoxide was introduced by initial

(10) (a) Aida, T.; Akihiko, T.; Fuse, M.; Inoue, S. *J. Chem. Soc., Chem Commun.* **1988**, 391. (b) Kroon, J. M.; Schenkels, P. S.; Van Dijk, M.; Sudhölter, J. R. *J. Mater. Chem.* **1995**, *5*, 1309.

(11) Schultz, R. A.; White, B. D.; Dishong, D. M.; Arnold, K. A.; Gokel, G. W. *J. Am. Chem. Soc.* **1985**, *107*, 6659.

(12) Watanabe, M.; Wooster, T. T.; Murray, R. W. *J. Phys. Chem.* **1991**, *95*, 45.

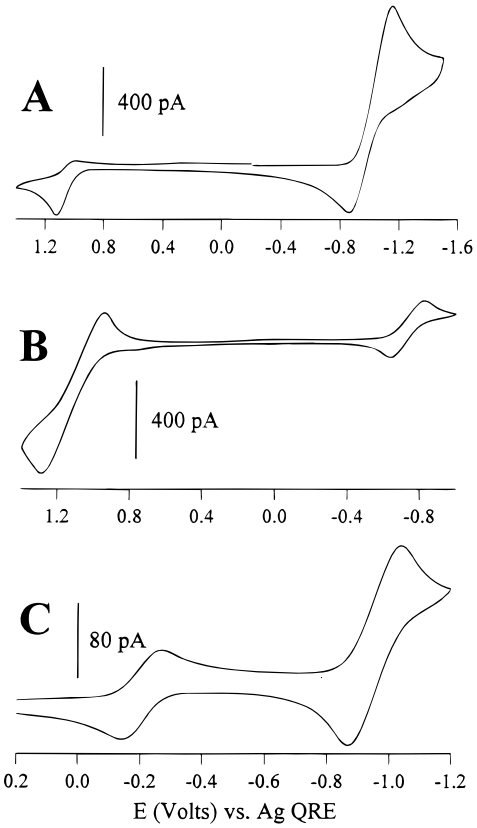

Figure 1. Cyclic voltammograms (20 mV/s) in undiluted room temperature melts, all containing 1.2 M $LiClO_4$: (A) T550PP, (B) Co(T550PP), and (C) Fe(T550PP)-Cl. The microelectrode radius is 5.0 μm.

evacuation of the cell, which was then backfilled with carbon monoxide. For experiments involving pyridine, use of a flow-through electrochemical cell allowed a ligand-containing gas to pass directly over a thin (~60 μm) porphyrin film.

Electrochemical Measurements. Potential scan voltammetric and potential step chronoamperometric experiments were performed with a high current sensitivity potentiostat of local design operating under computer control. Data acquisition was accomplished through a Keithley DAS-HRES 16-bit analog input/output board in an IBM 386-33 computer with locally written software. Microelectrode potential sweep voltammetry was used to assess the redox potentials of the porphyrin reactions. The apparent diffusion coefficients, D_{APP}, were determined with potential step chronoamperometry, analyzing the resulting current−time curves according to the Cottrell equation for linear diffusion.[13]

Results and Discussion

Microelectrode Voltammetry and Chronoamperometry in Undiluted Melts. Examples of microelectrode voltammetry in undiluted MePEG-porphyrin melts containing 1.2 M $LiClO_4$ are shown in Figure 1. The redox reactions to which the observed voltammetric peaks are assigned are based on previous observations of tetraphenylporphyrin complexes[4,5] in dilute, fluid solutions. The voltammetric oxidation and reduction waves in the free base T550PP melt (Figure 1A) correspond to ring oxidation and reduction, neither of which are completely chemically reversible, the ring oxidation least so. Voltammetry of the cobalt metalated melt Co(T550PP) (Figure 1B) displays a chemically reversible reduction at −0.75 V (formal potentials are averages of $E_{PEAK,OX}$ and $E_{PEAK,RED}$), which is assigned to the Co(II/I) reaction, and an oxidation wave at *ca.* +1.10 V, which is assigned to the porphyrin ring oxidation. The Co(III/II) reaction gives small, broad peaks in the 0 to +0.8 V potential range (these small currents are barely discernible on the scale of Figure 1B; on an expanded scale the oxidation peak current is ~21 pA). Co(III/II) porphyrin reactions are known to have very sluggish charge transfer kinetics and highly irreversible voltammetry is common, particularly in a solvent that is not strongly coordinating.[5] The iron metalated melt, Fe(T550PP)-Cl, exhibits waves (Figure 1C) at *ca.* −0.20 and −0.95 V which are assigned, respectively, to the Fe(III/II) and Fe(II/I) reactions. It is evident that, although the voltammetric reactions in Figure 1 are *all* ostensibly one electron reactions, there are wide variations in the observed currents.

Table 1. Diffusion Coefficients, Rate Constants, and Activation Parameters for MePEG-Porphyrins

reaction[a]	$[LiClO_4]$ (M)	D_{APP} ($cm^2\ s^{-1}$)[b]	k_{EX} ($M^{-1}\ s^{-1}$)[c]	E_{ACT} (kJ mol^{-1})[d]	A ($M^{-1}\ s^{-1}$)[e]
Co(II/I)	0.4	8.8×10^{-10}	5.2×10^5	50	1×10^{14}
Fe(II/I)	0.4	2.7×10^{-10}	1.6×10^5		
Fe(III/II)	0.4	2.9×10^{-10}	1.7×10^5	47	3×10^{13}
$T550PP^{0/\bullet -}$	1.2	6.2×10^{-9}	3.6×10^6	40	8×10^{13}
$T550PP^{0/\bullet +}$	1.2	(9.8×10^{-10})	$(5.5 \times 10^5)^f$	$(55)^f$	$(6 \times 10^{15})^f$
Co(II/I)	1.2	2.4×10^{-10}	1.2×10^5	49	6×10^{13}
Co(II/III)	1.2	2.6×10^{-12}			
Fe(II/I)	1.2	6.9×10^{-11}	3.7×10^4		
Fe(III/II)	1.2	2.2×10^{-11}	1.1×10^4	58	2×10^{14}
Co(II/I)	1.6	3.3×10^{-11}	1.9×10^4	65	1×10^{14}
Co(II/III)	1.6	5.5×10^{-13}			
Fe(II/I)	1.6	3.9×10^{-11}	2.2×10^4		
Fe(III/II)	1.6	3.4×10^{-12}	1.7×10^3	72	3×10^{13}

[a] $T550PP^{0/\bullet -}$ denotes the first reduction of the porphyrin ring; $T550PP^{0/\bullet +}$ denotes the first oxidation of the porphyrin ring. [b] D_{APP} for the Co(II/III) reaction is estimated from potential sweep voltammetry by using the treatment for charge transfer irreversible electrochemical reactions. All other D_{APP} values were determined by chronoamperometry. [c] Calculated from eq 1, taking $D_{PHYS} = D_{APP}$ for the Co(II/III) reaction, and $\delta = 16$ Å and $C = 0.40$ M. [d] Calculated from plots like Figure 3, where E_{ACT} = slope × R × 2.303. Temperature-dependent data could not be obtained for the Fe(II/I) reaction due to the long-term instability of the Fe(II) state in the Fe(T550PP)-Cl films. [e] Intercepts of plots in Figure 3 in terms of k_{EX}. [f] Data for $T550PP^{0/\bullet +}$ are uncertain due to chemical irreversibility, see Figure 1A.

The differing currents for the waves in Figure 1 represent differing rates of charge transport to the microelectrode surface, i.e., different apparent diffusion coefficients, D_{APP}. D_{APP} values for each reaction were assessed by potential step chronoamperometry, except for that of Co(III/II), which was evaluated from potential sweep voltammetry by using theory for a charge transfer irreversible reaction. Table 1 shows the results; the D_{APP} results vary with the concentration of dissolved $LiClO_4$ electrolyte as well as with the reaction. At 1.2 M $LiClO_4$, the chronoamperometrically measured D_{APP} values span a 3×10^3-fold range, from 6.2×10^{-9} $cm^2\ s^{-1}$ for the ring reduction of T550PP to 2.2×10^{-11} $cm^2\ s^{-1}$ for the Fe(III/II) reduction in the Fe(T550PP)-Cl melt to *ca.* 2.6×10^{-12} $cm^2\ s^{-1}$ for the Co(III/II) reaction in the Co(T550PP) melt.

Given their structural similarities, all of the MePEG-porphyrins, from free base to Co, should exhibit similar rates of physical self-diffusion (D_{PHYS}) in their undiluted phases. The differences in the D_{APP} values can accordingly be ascribed to differences in electron self-exchange enhancement of charge transport in the mixed valent diffusion layers around the electrode interfaces. The coupling of mass transport and electron hopping is described by the Dahms and Ruff equation,[14] which in corrected form is

$$D_{APP} = D_{PHYS} + \frac{k_{EX}\delta^2 C}{6} \qquad (1)$$

where k_{EX} ($M^{-1}\ s^{-1}$) is the electron self-exchange rate constant,

(13) (a) $I = nFAD_{APP}^{1/2}C/\pi^{1/2}t^{1/2}$. (b) Bard, A. J.; Faulkner, L. R. *Electrochemical Methods*; John Wiley & Sons; New York, 1980; p 143.

δ (cm) the site center-to-center spacing at electron transfer, and C the molar concentration of the electroactive species. The equation shows that for melts of similar structure (i.e., similar D_{PHYS}, δ, and C), variations in D_{APP} can be ascribed to variations in the electron self-exchange dynamics, and that D_{APP} is largest for redox couples with very fast electron self-exchanges, and closest to D_{PHYS} for redox couples with very slow electron self-exchanges. The latter is clearly the Co(III/II) couple; electrode kinetics for the latter reaction are known to be slow,[5] and indeed in a porphyrin redox polymer film we have previously witnessed[15] the inability of the Co(III/II) tetraphenylporphyrin self-exchange reaction to support charge transport at all.

Taking the Co(III/II) reaction as measuring D_{PHYS}, values of k_{EX} are accordingly calculated (Table 1) at 1.2 and 1.6 M $LiClO_4$ for the various porphyrin redox couples with eq 1. A Co(III/II) D_{PHYS} measurement was not accomplished in the melt containing 0.4 M $LiClO_4$ electrolyte; however, considering its essentially negligible values at the other electrolyte concentrations, it was assumed negligible in comparison to D_{APP} for the purpose of evaluation of k_{EX} for the redox couples studied there. The other parameters employed in the calculation of k_{EX} are $\delta = 16$ Å and $C = 0.40$ M;[16] the former value is based on a simple cubic lattice model and the measured porphyrin site concentration. All of the k_{EX} results are subject to some underestimation since a cubic lattice is obviously approximate for the porphyrinic shape, so the site−site separations at electron transfer may be somewhat smaller than the 16 Å value used. The uncertainty from this quarter is probably less than a factor of 2. The experimental uncertainty in D_{PHYS} arising from the poor quality of the Co(III/II) voltammetry is of minor consequence since even a 2-fold error in the Co(III/II) D_{PHYS} value causes only a 20−30% over-estimate of Fe(III/II) k_{EX}, and less for the other couples. Finally, no attempt has been made to correct for coupling between electron hopping and supporting electrolyte ion transport (electron migration[9a,17]), which if the latter is too slow can accelerate electron hopping, and it is possible that the k_{EX} of the most facile reactions have been somewhat over-estimated. Further study of the details of ion transport (and ion pairing) in these media will be necessary to evaluate the latter possibility.

Considering the k_{EX} results in Table 1 at 1.2 M electrolyte concentration, the ring-centered electron transfers are clearly the most facile. The rate difference between the ring cation radical and anion radical couples may be erroneous since the chemical irreversibility of the former would deplete the mixed valency in the diffusion layer and thereby depress the degree of charge transport enhancement. The rate constants k_{EX} (and activation parameters, see below) for the ring oxidation are accordingly shown in parentheses. The ring reduction rate is *ca*. 12-fold larger than the metal-centered Fe(II/I) and Co(II/I) reductions, which have similar rates.

There are limited literature data[18] with which to compare the Table 1 results. The rate constants fall into the same order as available electrochemically-derived heterogeneous electron transfer rate constants (k_S) for monomeric metalloporphyrins, namely[4,5,19] porphyrin ring > Co(II/I) ≈ Fe(II/I) > Fe(III/II). Other literature data include those by White and Murray[20] for steady state measurements on acetonitrile-bathed films of electrochemically polymerized metallotetrakis(*o*-aminophenyl)porphyrins, which gave $k_{EX} = 5 \times 10^6$, 4×10^4, 2×10^4, and 2×10^4 M^{-1} s^{-1} for the porphyrin ring reduction, the Co(II/I) reaction, the Fe(II/I) reaction, and the Fe(III/II) reaction, respectively. These values, which have been multiplied by six since that factor was omitted in the previous work,[20] are, with the exception of the Co(II/I) result, remarkably close to the results in Table 1 at 1.2 M $LiClO_4$.

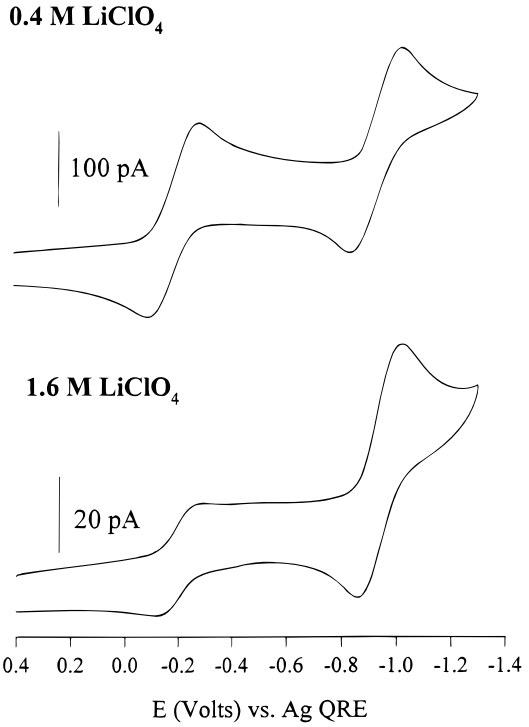

Figure 2. Cyclic voltammograms (20 mV/s) for Fe(T550PP)-Cl melt containing 0.4 M $LiClO_4$ and 1.6 M $LiClO_4$. The microelectrode radius is 5.0 μm.

The k_{EX} results generally decrease, however, with increasing concentration of $LiClO_4$ electrolyte added to the MePEG-porphyrin melt. Figure 2 illustrates the electrolyte dependency with microelectrode voltammetry observed in the Fe(T550PP)-Cl melt at 0.4 and 1.6 M $LiClO_4$ electrolyte concentrations. The activation results in Table 1 (*vide infra*) indicate that the decreases in room temperature k_{EX} generally correlate with increases in the activation barrier energies with increasing electrolyte concentration. The detailed reason for this dependency is not understood. Similar electrolyte concentration-induced variations of electron transfer rate also occur in polyether-tailed metal bipyridine complex melts;[21] there also, the change in k_{EX} could be assigned to increases in activation barrier energy (as opposed to the pre-exponential term of the rate expression).

Charge Transport Activation. The temperature dependence studies of D_{APP} values did not include the Co(III/II) couple so those data are examined as an Arrhenius activation plot by using $\log[D_{APP}]$ rather than $\log[k_{EX}]$ (Figure 3). Our experience[3,9] in

(14) (a) Dahms, H. *J. Phys. Chem.* **1968**, *72*, 362. (b) Ruff, I.; Friedrich, V. J. *J. Phys. Chem.* **1971**, *75*, 3297. (c) Ruff, I.; Friedrich, V. J.; Demeter, K.; Csaillag, K. *J. Phys. Chem.* **1971**, *75*, 3303. (d) Ruff, I.; Botar, L. *J. Chem. Phys.* **1975**, *83*, 1292. (e) Ruff, I.; Botar, L. *Chem. Phys. Lett.* **1986**, *126*, 348. (f) Ruff, I.; Botar, L. *Chem. Phys. Lett.* **1988**, *149*, 99.

(15) Karen Pressprich, Ph.D. Thesis, University of North Carolina at Chapel Hill, Chapel Hill, NC 1989.

(16) *C* was calculated from density measurements, which were obtained by weighing 1 μL capillaries filled with the MPEG-porphyrin.

(17) (a) Andreiux, C. P.; Saveant, J. M. *J. Phys. Chem*, **1988**, *92*, 6761. (b) The available ionic conductivity data for the porphyrin melts is scanty; a crude estimate from it gives an electrolyte ion diffusion coefficient in the 10^{-10} cm^2/s range for 1.2 M electrolyte.

(18) (a) Shirazi, A.; Barbush, M.; Ghosh, S.; Dixon, D. W. *Inorg. Chem.* **1985**, *24*, 2495. (b) Chapman, R. D. *J. Am. Chem. Soc.* **1982**, *104*, 1575. (c) Pasternack, R. F.; Spiro, E. G. *J. Am. Chem. Soc.* **1978**, *100*, 968.

(19) Chang, D.; Malinski, T.; Ulman, A.; Kadish, K. M. *Inorg. Chem.* **1984**, *23*, 817.

(20) White, B. A.; Murray, R. W. *J. Am. Chem. Soc.* **1987**, *109*, 2576.

(21) (a) Williams, M. E.; Lyons, L.; Long, J. W.; Murray, R. W. *J. Phys. Chem.*, in press. (b) Long, J. W. Unpublished results.

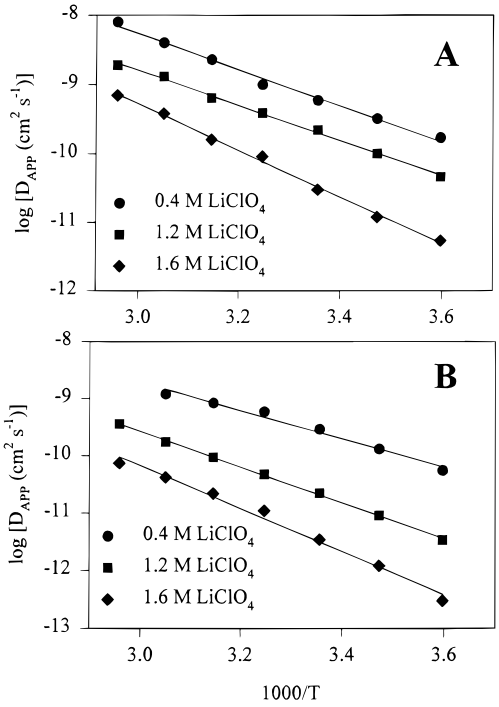

Figure 3. Activation plots for the (A) Co(II/I) and (B) Fe(III/II) porphyrin couples.

hybrid redox polyether melts has been that activation plots of physical diffusion coefficients are typically curved and those where charge transport is dominated by electron self exchanges are linear. The activation plots in Figure 3 are reasonably linear, indicative of the latter condition. Values of activation barriers and intercepts are given in Table 1. The E_{ACT} values are large, ranging for the Fe(III/II) couple from 47 kJ mol^{-1} at 0.4 M $LiClO_4$ to 72 kJ mol^{-1} at 1.6 M $LiClO_4$, as are (ignoring the parenthetical entry) the activation plot intercepts which are in the 10^{13}-10^{14} M^{-1} s^{-1} range.

As discussed in recent activation studies on metal bipyridine hybrid redox polyethers,[9a,b] activation barrier energies measured from rate constants obtained with eq 1 represent free energy barriers $\Delta G^{\neq}$ since the reactions are self-exchanges and work terms are unimportant (the reaction sites are in proximal contact already). Thus in the context of the classical relation[22]

$$k_{EX} = K_A \kappa \nu \exp\left[-\frac{\Delta G^*}{k_B T}\right] \qquad (2)$$

where K_A is the donor−acceptor precursor complex formation constant (estimated for the porphyrin−polyether as 1.5 M),[22] ν is the frequency factor, and κ is the electronic factor or transmission coefficient. The near-unity value of K_A means that the activation plot intercepts (A) in Table 1 can be equated with $\kappa\nu$ (s^{-1}) of eq 2. Since a reaction with $\kappa\nu \approx 10^{13}$ s^{-1} is considered to be adiabatic,[22] the intercepts in Table 1 imply that the electron transfers in the porphyrin melts are highly adiabatic.

The activation results, i.e., large activation barrier energies and adiabatic-like pre-exponential terms, are very similar to those obtained in activation studies on metal bipyridine hybrid redox polyethers,[9a,g,21] where large activation barrier energies and adiabatic-like pre-exponentials were also found in measurements of Fe(III/II), Co(II/I), Ru(III/II), and Ru(II/I) electron self-exchange rates. Finding the same behavior with a different class of redox moieties suggests the possibility of a general explanation in the semisolid, concentrated hybrid redox polyether melts.

Theoretical studies[23] connected with solvent dynamics behavior (in fluid media) have pointed out the possible role of strong friction forces (slow energy relaxation in solvent vibrational modes) in confining nuclear coordinates in the barrier-top region for sufficiently long times as to force adiabatic behavior on an otherwise non-adiabatic electron transfer reaction. We speculate that the electron transfers in the semisolid hybrid redox polyether melts may be influenced by long dwell times in the barrier-top region. This possibility will be considered in further studies of these unusual materials.

Axial Ligation of MPEG-Porphyrin Films. Redox potentials for metal-centered metalloporphyrin reactions vary with the state of axial coordination. The formal potential of the Fe(III/II) reaction in dilute, fluid solutions of the metalloporphyrin Fe(TPP)-Cl depends on the solvent; its shift to more positive values in coordinating solvents such as DMSO is accounted for by stabilization of the Fe(II) state. In contrast, the formal potential of the Fe(II/I) reaction of the same metalloporphyrin in dilute solutions is relatively insensitive to the ligating environment. The difference ($\Delta E^{o\prime}$) between the Fe(III/II) and Fe(II/I) formal potentials is consequently a measure of the coordinating propensity of the solvent medium; in a noncoordinating solvent such as CH_2Cl_2, $\Delta E^{o\prime} = 0.77$ V, in DMSO, $\Delta E^{\circ} = 1.03$ V.[4b] The spacing between the two waves in the Fe(T550PP)-Cl melt (Figure 1C) is 0.76 V. By comparison to the dilute solution behavior, the MePEG chains attached to the porphyrin must bath it in a relatively noncoordinating, polyether "solvent". Thus, the addition of other axial ligands to the porphyrin melt should lead to observable changes in the potential of the Fe(III/II) reaction in the melt phase.

As solid-state voltammetric studies have previously illustrated,[2b,24] nonvolatile solvents (such as polyethers and the present melts) allow volatile reagents to be introduced into and removed from the investigated phase by partition at the melt/gas interface. The selectivity of the axial coordination chemistry of the metalloporphyrins has potential usefulness in gas analysis. The two following preliminary results demonstrate that changes in axial ligation in the metallo-MePEG-porphyrin melt phase can be detected. Fuller descriptions will follow in subsequent papers.

Figure 4 shows Fe(III/II) voltammetry of the Fe(T550PP)-Cl melt (as a thin film covering the microelectrode) bathed first in a stream of dry N_2 (—) and then (- - -) in N_2 containing pyridine vapor at 10% of its saturation level (at room temperature). The Fe(III/II) wave in dry N_2 is essentially the same as seen in Figure 1C. Exposure to pyridine vapor, after a period of equilibration, results in a 0.335-V shift of a portion of the Fe(III/II) wave to a more positive potential (Figure 4 (- - -), from −0.190 to +0.145 V). The shift is as expected[4] (from fluid solution results) for stronger coordination of the Fe(II) than the Fe(III) state. The formal potential of the Fe(III/II) reaction in dilute solutions of the metalloporphyrin Fe(TPP)-Cl shifts positively by 0.47 V in pyridine solvent as compared to CH_2Cl_2 solvent.[4a]

The relative magnitude of the pyridine-coordinated and noncoordinated Fe(III/II) waves in Figure 4 (- - -) indicates that

(22) Newton, M. C.; Sutin, N. *Annu. Rev. Phys. Chem.* **1984**, *35*, 437.

(23) (a) Mikkelsen, K. V.; Ratner, M. A. *Chem. Rev.* **1987**, *87*, 113. (b) Heitele, H. *Angew. Chem., Int. Ed. Engl.* **1993**, *32*, 359. (c) Calef, D. F.; Wolynes, P. G. *J. Phys. Chem.* **1983**, *87*, 3387. Calef, D. F.; Wolynes, P. G. *J. Chem. Phys.* **1983**, *78*, 470.

(24) (a) Barbour, C. J.; Parcher, J. F.; Murray, R. W. *Anal. Chem.* **1991**, *63*, 604. (b) Parcher, J. F.; Barbour, C. J.; Murray, R. W. *Anal. Chem.* **1989**, *61*, 584. (c) Geng, L.; Longmire, M. L.; Reed, R. A.; Parcher, J. F.; Barbour, C. J.; Murray, R. W. *Chem. Mater.* **1989**, *1*, 58. (d) Hardy, L. C.; Shriver, D. F. *J. Am. Chem. Soc.* **1985**, *107*, 3823.

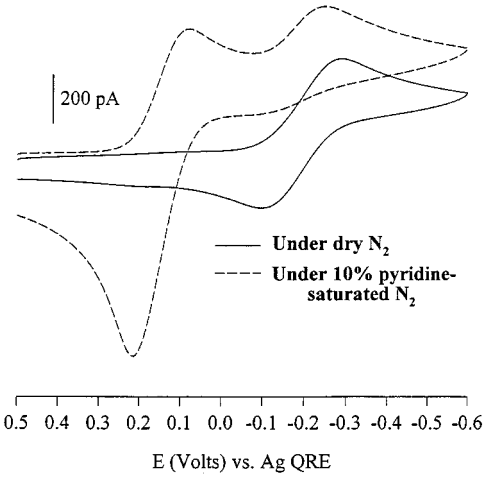

Figure 4. Cyclic voltammograms (50 mV/s) for the Fe(T550PP)-Cl, Fe(III/II) couple (solid line) under a flow of dry N_2 and (dashed line) under a flow of 10% pyridine-saturated N_2 following equilibration for 15 min with use of a 25 μm radius micro disk working electrode and 1.2 M $LiClO_4$.

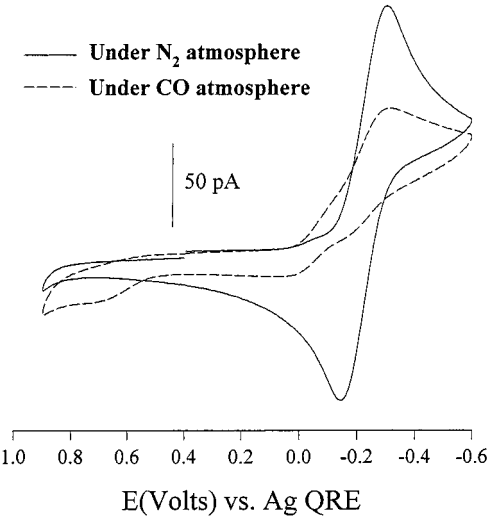

Figure 5. Cyclic voltammograms (50 mV/s) for the Fe(T550PP)-Cl, Fe III/II couple (solid line) under a N_2 atmosphere and (dashed line) under a CO atmosphere with use of a 5.0 μm radius microdisk working electrode and 0.4 M $LiClO_4$.

roughly 0.2 M pyridine was partitioned into the melt film as an axial ligand. Additional pyridine appears also to partition into the polyether "solvent" part of the melt, since the voltammetric currents exhibit a general increase. The increase in current is understood as a diffusion-plasticizing effect of the pyridine, which is a phenomenon seen before in other polyether phase solid-state voltammetry[2b,24] studies where the redox moiety was a dilute solute and electron self-exchanges were thus unimportant.

The pyridine coordination in Figure 4 (- - -) can be reversed. Bathing the melt film under a stream of dry N_2 for several hours causes the Fe(III/II) voltammetry to revert completely to its original state (i.e., Figure 4 (—)). In a future publication we will address the dynamics for de-complexation of Fe(T550PP)-Cl and of Co(T550PP) melts with pyridine and other strong axial ligands.

Carbon monoxide forms both mono- and bis-adducts with the Fe(II) state of iron metalloporphyrins[25] in dilute, fluid solution, but is inactive toward the Fe(III) state. Figure 5 (- - -) shows the consequences of exposing a Fe(T550PP)-Cl melt film to a CO atmosphere. The change in voltammetry from that seen under N_2 is very rapid; the Fe(III/II) reaction becomes irreversible and a small oxidation peak appears at *ca.* +0.6 V. The voltammetry quickly reverts to the original (—) when the film is placed under vacuum to remove the CO.

The voltammetry in Figure 5 for the Fe(T550PP)-Cl melt in the presence of CO is entirely consistent with the behavior of dilute solutions of Fe(TPP)-Cl in a noncoordinating solvent.[24] The electrochemically generated Fe(II) state strongly binds CO, stabilizing the resulting adduct toward oxidation, which in Figure 5 occurs at +0.6 V.

These two examples demonstrate that axial coordination chemistry familiar for dilute solutions of iron metalloporphyrins in fluid solvents can also be seen, in qualitatively similar form, in the semisolid, concentrated melt phase of the Fe(T550PP)-Cl MePEG-porphyrin. One infers then that other interesting axial ligation-based chemistry of metallporphyrins can be accessed in the semisolid melt states generated by their redox polyether hybrids.

Acknowledgment. This research was supported in part by grants from the Department of Energy and the National Science Foundation. I.K.K. thanks the Basic Science Research Institute Program (BSRI-96-3430) of the Ministry of Education, Korea, for support.

JA972081D

(25) Swistak, C.; Kadish, K. M. *Inorg. Chem.* **1987**, *26*, 405.